NASA TECHNICAL
MEMORANDUM

NASA TM-73865

(NASA-TM-73865) CHARGING OF FLEXIBLE SOLAR ARRAY SUBSTRATES IN KILOVOLT ELECTRON BEAMS (NASA) 32 p HC A03/MF A01 CSCL 10A

N78-21199

Unclas
G3/18 12427

NASA TM-73865

CHARGING OF FLEXIBLE SOLAR ARRAY SUBSTRATES IN KILOVOLT ELECTRON BEAMS

by John V. Staskus and Steven J. Narciso
Lewis Research Center
Cleveland, Ohio 44135
March 1978

1. Report No.	2. Government Accession No.	3. Recipient's Catalog No.
NASA TM-73865		
4. Title and Subtitle CHARGING OF FLEXIBLE SOLAR ARRAY SUBSTRATES IN KILOVOLT ELECTRON BEAMS		5. Report Date 6. Performing Organization Code
7. Author(s) John V. Staskus and Steven J. Narciso		8. Performing Organization Report No. E-9455 10. Work Unit No.
9. Performing Organization Name and Address National Aeronautics and Space Administration Lewis Research Center Cleveland, Ohio 44135		11. Contract or Grant No. 13. Type of Report and Period Covered Technical Memorandum
12. Sponsoring Agency Name and Address National Aeronautics and Space Administration Washington, D.C. 20546		14. Sponsoring Agency Code
15. Supplementary Notes		

16. Abstract

A series of survey tests were conducted in the NASA-Lewis Research Center Geomagnetic Substorm Simulation Facility to evaluate samples of flexible solar arrays supplied by the COMSAT Corporation. The samples used woven carbon fibers and/or coatings to increase the surface conductivity of the KAPTON substrate and thereby reduce surface charging. Four different samples were evaluated by exposing them to monoenergetic electron beams of 2 to 20 KeV at a current density of 1 nA/cm^2. Simulated eclipse tests were also conducted. The results were as expected; the more continuous the conductive pattern, the lower the surface charging.

17. Key Words (Suggested by Author(s))	18. Distribution Statement
Solar arrays Spacecraft construction materials Electrostatic charging	Unclassified - unlimited STAR Category 18

19. Security Classif. (of this report)	20. Security Classif. (of this page)	21. No. of Pages	22. Price*
Unclassified	Unclassified		

* For sale by the National Technical Information Service, Springfield, Virginia 22161

CHARGING OF FLEXIBLE SOLAR ARRAY SUBSTRATES IN KILOVOLT ELECTRON BEAMS

by John V. Staskus and Steven J. Narciso

National Aeronautics and Space Administration
Lewis Research Center
Cleveland, Ohio 44135

E-9455

INTRODUCTION

Many satellites in geosynchronous orbit have experienced anomalous behavior in electronic systems at some time during their operational life[1,2]. The anomalies are believed to be the result of discharges which occur following the differential charging of various spacecraft surfaces by the geomagnetic substorm environment[3]. Investigations to determine the behavior of various materials under charging conditions have been undertaken in the Lewis Research Center's geomagnetic substorm simulation facility[4]. Thermal control materials and some solar array segments have undergone considerable testing[5,6,7]. These samples all discharged under conditions simulating moderate to severe substorms.

Flexible substrate solar arrays used on some communications satellites present a large insulator area that can be charged by the environment. The first such array was designed and built for the Canadian-American Communications Technology Satellite (CTS) before spacecraft charging effects were understood. There was sufficient concern for the possible charging of this AEG-Telefunken supplied array that a charging investigation was conducted[8]. The CTS has survived the environmental charging since launch in January, 1976, but has suffered a power loss possibly due to a charging event[9].

When a similar solar array was proposed for use on the latest COMSAT satellite, Intelsat V, several modifications to the substrate were suggested to minimize the charging of the dielectric surface. The KAPTON-fiberglass substrate was changed to include woven carbon fiber fabrics and/or conductive surface coatings. The fabric and coatings would be electrically grounded. These "quasiconductive" dielectric substrates required testing to evaluate their effectiveness in controlling surface charging. Four solar array segments were prepared by AEG-Telefunken and COMSAT using different carbon fabric weaves and surface coatings.

The segments were tested in the Lewis Research Center facility as part of the continuing evaluation of new materials and techniques being developed to control surface charging. Survey tests were conducted on both the solar array sides and the substrate sides by exposure to 2 to 20 KeV electron beams. Simulated eclipse testing was also conducted in which the segments were exposed periodically to sunlight while being irradiated by the electron beam. This report describes the testing and summarizes the results.

SAMPLE DESCRIPTIONS

All of the array segment samples were nominally 10 centimeters by 11 centimeters in size. The solar cells were 2 centimeters by 4 centimeters having 10 Ω-centimeters resistivity. The substrates were composed of 12.5 μm thick (0.0005 in.) KAPTON sheet (19 gm/m^2) reinforced with either a woven carbon fiber fabric or a woven glass fiber fabric. The samples were designated set 1, set 2, set 3, and set 4 by COMSAT Corporation. Table I summarizes the characteristics of the sample substrates.

The set 1 sample, fig. 1, had a carbon fiber fabric of 66 gm/m^2 density bonded to the KAPTON sheet for reinforcing and charge control. The elements of the woven carbon fiber fabric were approximately 1.5 mm wide and spaced 5 per centimeter resulting in an open area of about 6 percent. A conductive strip down each edge of the rear surface provided the electrical contact with the carbon fiber reinforcing and charge control material. A short piece of KAPTON insulated wire was epoxied to each strip for circuit connections. The eight 2×4 centimeter solar cells were mounted on the KAPTON with RTV 566 in two parallel strings of four cells in series. The 0.1 mm thick cerium doped cover slides were applied with DC 9350 adhesive and were similar to those used on the Communications Technology Satellite.

The set 2 sample, fig. 2, had 45 gm/m^2 carbon fiber fabric bonded to the KAPTON sheet for reinforcing and charge control. The fabric elements were about 1 mm wide and spaced about $3\frac{1}{2}$ per centimeter resulting in an open area of about 42 percent. Electrical connection to the carbon fiber fabric was provided by a conductive strip down each edge of the sample's rear surface. A short length of silver mesh was bonded to each strip for solder connections. The four 2 centimeter by 4 centimeter solar cells, connected in series, were centered on the KAPTON substrate. The long dimensions of substrate and cells were parallel. The 0.15 mm thick cerium doped cover slides had a magnesium fluoride anti-reflection coating.

The set 3 sample, fig. 3, was similar to the set 2 sample except that a film of adhesive-soot material was applied over the woven carbon fiber. This was done to improve conductivity and thereby reduce the charge buildup.

The set 4 sample, fig. 4, had a substrate of KAPTON reinforced with 27 gm/m^2 woven glass fiber fabric. The weave density of about 24 strands per centimeter allowed very little, if any, open area. This sample had the reinforcing material applied to the front or solar cell side of the KAPTON sheet. The charge control material, a mixture of adhesive and soot, was applied to the bare KAPTON on the rear surface of the substrate. Conductive strips and silver mesh again provided electrical connection to the conductive coating on the rear of the substrate. The solar cells were the same type as used on the sets 2 and 3 samples.

DESCRIPTION OF TESTS

The test program consisted of three parts. In the first series of tests the sample front surfaces were exposed to the electron beam without solar simulation. In the second series of tests the backside surfaces were exposed and in the third series the front surfaces were exposed to the electron beam while being subjected to simulated solar illumination and eclipse. In the first two series of tests the samples were subjected to nominal electron fluxes of 1 nA/cm^2 for 20 to 30 minutes at each of the various electron beam accelerating voltages. In the third series of tests the electron flux was nominally 1 nA/cm^2 and the beam energy was 20 KeV. Each test was begun with the sample surface neutral. An ion source was used between tests to discharge this surface. The surface potential measuring system verified that the surface was neutral. The electron current collected by the solar cell circuit and that collected by the substrate were monitored separately. The sample surface potential profile was monitored using the electrostatic voltmeter which was swept across the surface at a minimum separation of about 0.2 centimeter. Discharge activity was monitored with a 15 centimeter diameter loop antenna centered about 38 centimeters from the sample center.

The first series of tests, run at beam voltages of 2, 5, 8, 10, 12, 14, 16, 18, and 20 KV, was conducted to survey the response of the front dielectric surface and the solar cells. The second series of tests, run at 2, 8, 12, 16, and 20 KV beam voltages, was conducted to survey the backside performance. The samples could be compared one to another to determine the most effective technique for controlling charge buildup on the rear surfaces.

In the third series of tests, the front surface of each sample was irradiated with a 1 nA/cm^2, 20 KeV electron flux for a period of two hours. The first half hour period was similar to the initial front surface tests except that the sample temperature was lowered to about -18^{o} C. During the second half hour the sample was illuminated by a solar simulator producing about 0.6 sun intensity at the sample plane. During the third half hour the sample was again in darkness while during the fourth half hour it was illuminated. Throughout the test the temperature, substrate collection current, cell circuit collection current, and surface potential profile were recorded once per minute. During the illuminated portions of the test, the array segment short circuit current and open circuit voltage were also recorded each minute.

DISCUSSION OF RESULTS

The test results for the set 2 sample is shown in figures 5 through 8. Figure 5 shows some typical surface potential profiles for the front and rear of sample 2. All are profiles of surfaces being bombarded in darkness. Figures 5(a) and (b) are equilibrium profiles of the front surface under exposure to 5 KeV (low energy) and 20 KeV (high energy) beams, respectively. Note that in the low energy beam, the KAPTON border becomes charged to a significantly higher potential than the cell cover slide. In the high energy beam the potentials of the cover slide and KAPTON border are comparable. Figures 5(c) and (d) show the rear surface in a high energy beam early in the test and at equilibrium. The carbon fiber threads of about 0.1 centimeter width and intervening 0.2 centimeter squares of KAPTON are resolvable as the alternating potential peaks and valleys. The conductive strips on the edges of the sample are seen as high potential peaks. The most significant observation to be made is that the small open areas of KAPTON on the rear surface become charged to nearly the same potential as the broad open KAPTON borders on the front surface. Therefore, it appears that the carbon fiber simply breaks up the charging into smaller areas.

Figure 6 shows the range of potentials occupied by the various surface materials of the sample for exposure to electron beams of 2 to 20 KeV energy. Figure 7 shows the equilibrium electron currents to the conductive substrate and solar cell circuits in beams of 2 to 20 KeV energy. It should be noted that increasing accelerating potentials focus the beam so that a 20 KeV beam of 1 nA/cm^2 density at the sample center will not provide the same total current to the sample as a 2 KeV beam of the same density at the sample center. The current collected by the solar cell circuit during electron irradiation of the substrate side is not shown since it was more than an order of magnitude less than the current collected during frontal irradiation. Figure 8 is a summary of the test conducted with the solar simulator. Figures 8(a) and (b) are records of the surface potentials on the cover slides and KAPTON substrate border. Note that under illumination of only 0.6 sun intensity the surface potentials are reduced by an order of magnitude from the values reached during electron irradiation in total darkness and may be due to the photo conductivity of KAPTON[10]. Figure 8(c) is a plot of sample temperature versus time. The thermocouple used to monitor the temperature was located in the center of the rear surface of the sample. Due to its location it probably indicated the true temperature of all surfaces of the sample only during the first half hour for which there were no thermal inputs to the sample and a steady state had been achieved. Figure 8(d) is a cumulative record of the discharge activity that took place during the test. The three counters connected to the loop antenna were operating with thresholds of 1V, 2V, and 5V. The curve labeled with roman numeral I shows the occurence of discharges which generated pulses of greater than 1V in the antenna. Curve II is for those discharges which induced pulses of greater than 2V and curve III is for pulses of greater than 5V. No discharges of level III were observed during the two hour test of sample of set 2 and only one was detected during each two hour test of samples of set 3, set 4, and set 1. Discharge activity was greatest during the first half hour when the sample was cold and in darkness. The discharge rate was reduced following illumination of the sample but increased during the second half hour of darkness. The discharge rate during the second dark period was somewhat less than the rate during the first half hour and may be due to the higher sample temperature. The discharge activity during the first and second test series is summarized in table II.

The test results obtained with the set 3 sample are summarized in figures 9 through 12. Figure 9 shows typical potential profiles for this sample. This sample was identical to the set 2 sample except for the addition of the soot bearing charge control material to the rear surface. The cover slide and KAPTON border potential profile for low energy (5 KeV) electron beam irradiation (fig. 9(a)) is very similar to that for the set 2 sample (fig. 5(a)). The profile for high energy (20 KeV) electron beam irradiation (fig. 9(b)) shows that the KAPTON border became less highly charged probably due to the additional adhesive-soot charge control material. The most dramatic improvement is noted in figure 9(c) which shows the profile of the rear surface exposed to a 20 KeV electron beam. The maximum potential is two orders of magnitude less than that of the sample lacking the adhesive-soot charge control material. Figures 10, 11, and 12 show the surface potentials versus beam energy, collected electron currents versus beam energy, and curves summarizing the two hour test in which the sample was illuminated by simulated solar radiation.

The test results obtained with the set 4 sample are summarized in figures 13 through 16. Figure 13(a) shows the front surface potential profile when exposed to a 5 KeV electron beam. The cover slide and fiberglass border became charged to approximately the same potentials as the cover slides and KAPTON borders of samples of sets 2 and 3. The potential profile of the surface exposed to a high energy (20 KeV) electron beam is shown in figure 13(b). Exposure of the rear surface to a 20 KeV beam produced the potential profile of figure 13(c). Recall that the rear surface has the adhesive-soot charge control material applied to plain KAPTON without any woven carbon fiber material. Comparison with figure 9(c) shows that the adhesive-soot material alone is nearly as effective as the combined woven carbon fiber and soot bearing material in reducing charge accumulation. Figures 14, 15, and 16 show the surface potentials versus beam energy, collected electron currents versus beam energy, and the curves summarizing the two hour test of alternating periods of darkness and simulated solar illumination.

The test results obtained with the sample of set 1 are summarized in figures 17 through 20. This sample was a better simulation of a proposed flight array in that the exposed area of the substrate on the solar cell side was a small fraction of the total sample area. Figure 17(a) shows the two deep potential wells due to charge accumulation on the narrow KAPTON borders. The potentials reached by the surfaces in the low (5 KeV) energy electron beam were much the same as the levels reached by similar surfaces on the other three samples. The voltage probe crossed four cover slides as it traversed the sample and evidence of these is barely discernable in the profile of figure 17(a). Figure 17(b) is a typical surface potential profile of sample 1 in a high energy (20 KeV) electron beam. The solar cell cover slides are more easily seen. The potential profile of the rear surface in a 20 KeV electron beam is shown in figure 17(c) The rear surface of this sample looks much like the rear of the set 2 sample except that the carbon fiber material is more densely woven. Comparison of figure 17(c) with figure 5(c) shows that the closer weave eliminated the numerous highly charged regions evident on the rear of sample 2. Although an improvement over the behavior of sample 2 was realized, the closer weave was not as effective in reducing charge accumulation as the soot bearing material applied to samples 3 and 4 (see figs. 9(c) and 13(c)). Figures 18, 19, and 20 show the surface potentials versus beam energy, sample currents versus beam energy and the data summarizing the two hour test with periods of solar simulation.

The discharge activity of the samples during the 20 to 30 minute tests in darkness is collected in table II. The numbers represent the cumulative number of discharges which induced signals of greater than 1V, 2V, and 5V in the loop antenna during 20 minutes of exposure to the electron beam. The set 1 sample experienced significantly more discharge activity on the front surface than the other three samples. This may be due to the larger number of solar cells whose cover slides could become charged and independently discharge to the solar cell interconnects. Comparison of figures 8(d), 12(d), 16(d), and 20(d) shows that illumination of the front surface significantly reduced or eliminated discharge activity on all samples which may be due to the photoconductivity of KAPTON[8]. The data in the table indicates that the densely woven carbon fiber fabric alone or the less dense carbon fiber fabric with the adhesive-soot material added were most effective in preventing discharge activity when the rear surface was irradiated in darkness.

CONCLUDING REMARKS

Four solar array segments of differing substrate construction supplied by the COMSAT Corporation, were exposed to monoenergetic electron beams in the Lewis Research Center electron irradiation facility. These segments differed in the approach used to (1) reinforce the basic KAPTON sheet substrate, and (2) to make the dielectric substrate "quasi-conductive" and hence, minimize surface charge build up.

The sample which exhibited the lowest surface potential on its rear surface was that with a woven carbon fiber reinforcing material (density of 45 gm/m^2) and an adhesive-soot mixture applied to the back (set 3). The sample having only the adhesive-soot mixture applied to the rear (set 4) ranked second. The set 1 sample, having only the higher density (66 gm/m^2) woven carbon fiber material on the back, ranked third in lowering substrate rear surface potentials and the sample having only the low density (45 gm/m^2) woven carbon fiber material (set 2) ranked last. These results are as expected; the more nearly continuous the "quasiconductive" layer, the lower the surface potential.

In terms of discharge activity on the rear surface, the set 1 and set 3 samples appear equivalent with no discharges recorded. Samples 2 and 4 did exhibit some discharge activity on the rear surface with sample 2 the most active.

The data obtained from these tests show that electronic charge accumulation by the substrates of flexible solar arrays can be reduced. This reduction can also be obtained with minimum impact on the solar array weight since some materials used for charge control also serve as strengthening elements in the flexible substrate. The influence of these charge control techniques on the thermal characteristics of the array have yet to be evaluated.

REFERENCES

1. Fredricks, R. W.; and Scarf, F. L.: Observation of Spacecraft Charging Effects in Energetic Plasma Regions. Photon & Particle Interactions with Surfaces in Space, R. J. L. Grard, ed., D. Reidel Publ. Co., 1973, pp. 277-308.

2. McPherson, D. A.; Cauffman, D. P.; and Schober, W. R.: Spacecraft Charging at High Altitudes: The Scatha Satellite Program. AIAA Paper 75-92, Jan. 1975.

3. Rosen, A.: Spacecraft Charging - Environment Induced Anomalies. AIAA Paper 75-91, Jan. 1975.

4. Berkopec, Frank D.; Stevens, N. John; and Sturman, John C.: The Lewis Research Center Geomagnetic Substorm Simulation Facility. NASA TM X-73602, 1976.

5. Stevens, N. John; Klinect, Vernon W.; and Berkopec, Frank D.: Environmental Charging of Spacecraft Surfaces: Tests of Thermal Control Materials for Use on the Global Positioning System Flight Space Vehicle, Part 1: Specimens 1-5. NASA TM X-73467, 1976.

6. Stevens, N. John; Berkopec, Frank D; and Blech, Richard A.: Environmental Charging of Spacecraft Surfaces: Tests of Thermal Control Materials for use on the Global Positioning System Flight Space Vehicle, Part 2: Specimens 6-9. NASA TM X-73436, 1976.

7. Stevens, N. John; et. al.: Testing of Typical Spacecraft Materials in a Simulated Substorm Environment. NASA TM X-73603, 1976.

8. Stevens, N. John; Lovell, Robert R.; and Gore, J. Victor: Spacecraft Charging Investigation for the CTS Project. NASA TM X-71795, 1975.

9. Stevens, N. John; Klinect, Vernon W.; and Gore, J. Victor: Summary of CTS Transient Event Counter Data After One Year of Operation. NASA TM X-73710, 1977.

REFERENCES

10. Coffey, H. T.; Nanevicz, J. E.; and Adamo, R. C.: Photoconductivity of High-Voltage Space Insulating Materials. (SRI Proj. 3545, Stanford Res. Inst.; NASA Contract NAS3-18912.) NASA CR 134995, 1975.

ORIGINAL PAGE IS
OF POOR QUALITY

TABLE I. - SUMMARY OF SAMPLE SUBSTRATE CHARACTERISTICS

Set number	Materials[1]	Weight: Elements (gm/m^2)	Weight: Substrate w/o Anti-charging (gm/m^2)	Dimension (mm)	Anti-charging represented by
1	KAPTON (12.5 μm) CFC[2] CY 209 Hardener HT 972	19 66 66	155	100 × 110	CFC
2	KAPTON (12.5 μm) CFC DuPont 46971 Hardener RC 805	19 45 31	95	100 × 110	CFC
3	KAPTON (12.5 μm) CFC DuPont 46971 Hardener RC 805	19 45 40	104	100 × 110	CFC + DuPont + Hardener + Soot
4	KAPTON (12.5 μm) Glass Fiber 90001 DuPont 46971 Hardener RC 805	19 27 13	59	100 × 110	DuPont + Hardener + Soot

[1] All of the samples had 2 strips of silver-filled polyester bonded to the rear surface so that the samples' rear side could be grounded. All of the samples were sent by AEG/Telefunken. Set 1 was received without cells and cells were mounted on the samples for COMSAT by TRW Space Systems.

[2] Carbon fiber composite (CFC).

TABLE II. - CUMULATIVE DISCHARGES AT 20 MINUTES

		Electron beam energy, KeV																	
		10			12			14			16			18			20		
		>1v	>2v	>5v	>1v	>2v	>5v	>1v	>2v	>5v	>1v	>2v	>5v	>1v	>2v	>5v	>1v	>2v	>5v
Frontal	1	1	0	0	6	1	0	6	3	0	11	3	0	5	4	0	16	4	2
irradiation	2	0	0	0	0	0	0	0	0	0	0	0	0	2	1	1	2	0	0
	3	0	0	0	0	0	0	0	0	0	0	0	0	2	0	0	7	0	0
	4	0	0	0	0	0	0	0	0	0	1	0	0	1	0	0	8	3	2
Rear	1	-	-	-	0	0	0	-	-	-	0	0	0	-	-	-	0	0	0
irradiation	2	-	-	-	0	0	0	-	-	-	1	0	0	-	-	-	5	1	0
	3	-	-	-	0	0	0	-	-	-	0	0	0	-	-	-	0	0	0
	4	-	-	-	0	0	0	-	-	-	0	0	0	-	-	-	3	1	0

ORIGINAL PAGE IS
OF POOR QUALITY

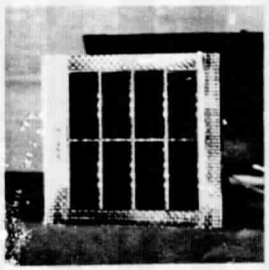

Front

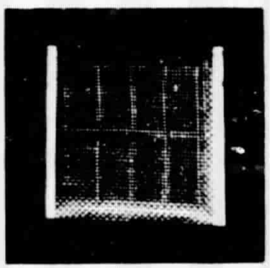

Rear

Figure 1. - Sample # 1.

Front

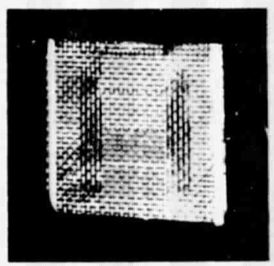

Rear

Figure 2. - Sample # 2.

Front

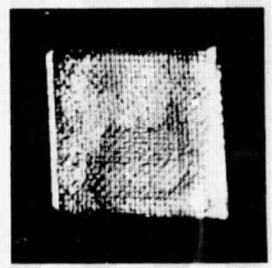

Rear

Figure 3. - Sample # 3.

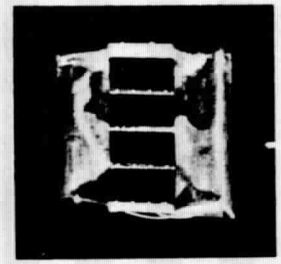

Front

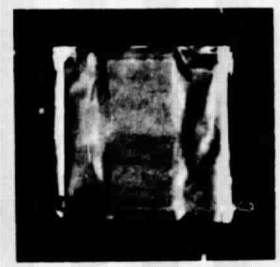

Rear

Figure 4. - Sample # 4.

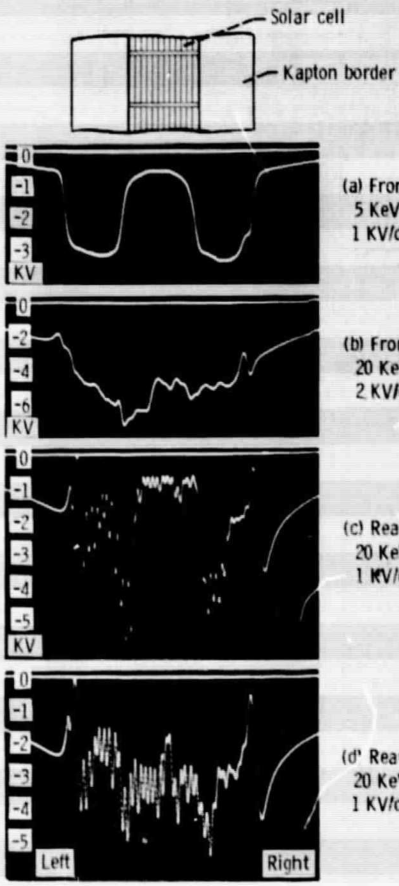

(a) Front surface potential profile, 5 KeV beam, minute 26, 1 KV/division.

(b) Front surface potential profile, 20 KeV beam, minute 20, 2 KV/division.

(c) Rear surface potential profile, 20 KeV beam, minute 1, 1 KV/division.

(d) Rear surface potential profile, 20 KeV beam, minute 20, 1 KV/division.

Figure 5. - Typical surface potential profiles of sample # 2.

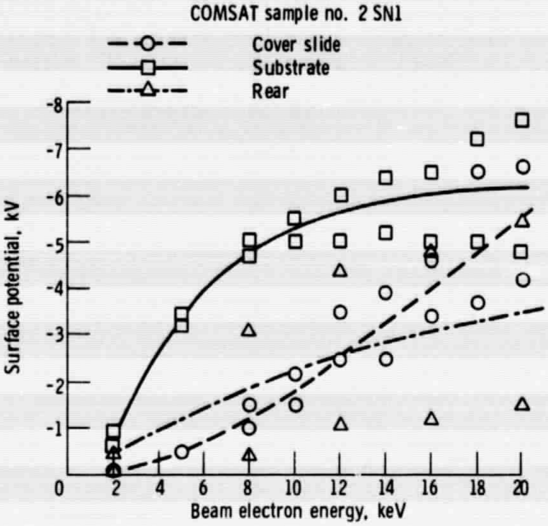

Figure 6. - Surface potential versus beam energy for sample no. 2.

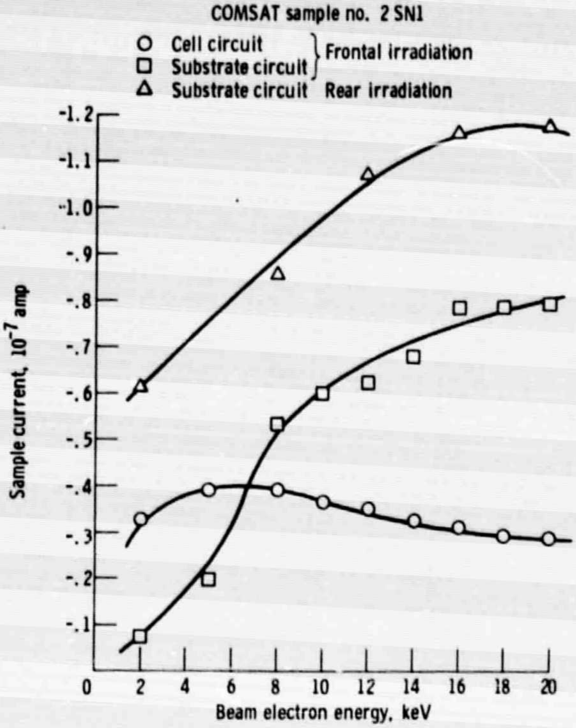

Figure 7. - Collected current versus beam energy for sample no. 2.

ORIGINAL PAGE IS OF POOR QUALITY

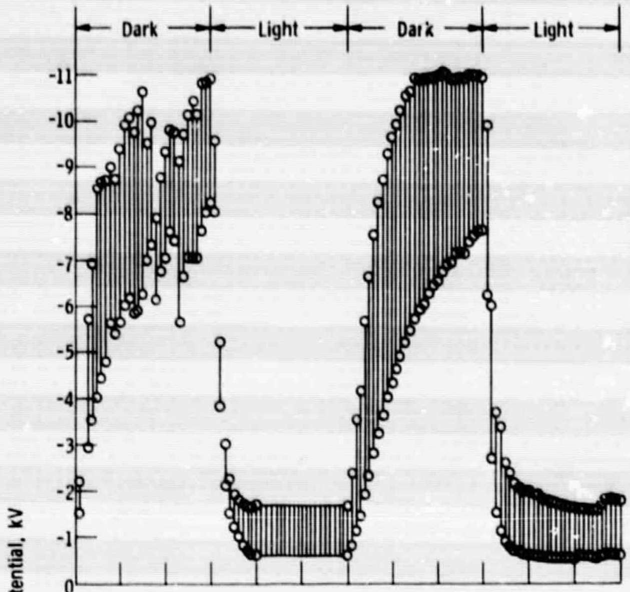

(a) Surface potential of solar cell cover slides versus time during solar simulation test of sample number 2.

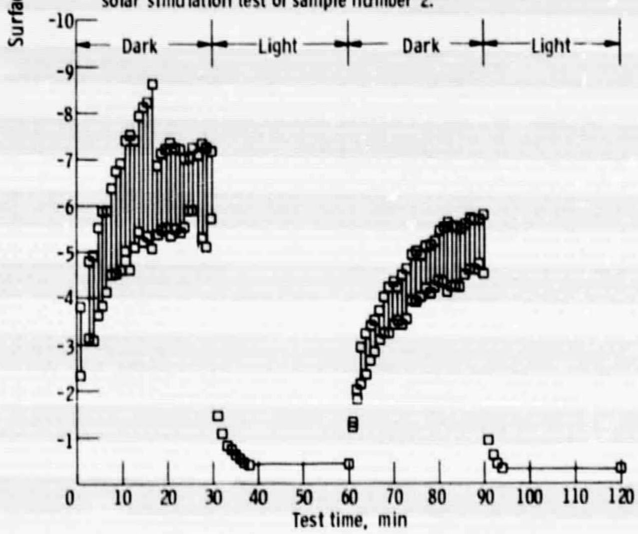

(b) Surface potential of KAPTON border around solar cells versus time during solar simulation test of sample number 2.

Figure 8.

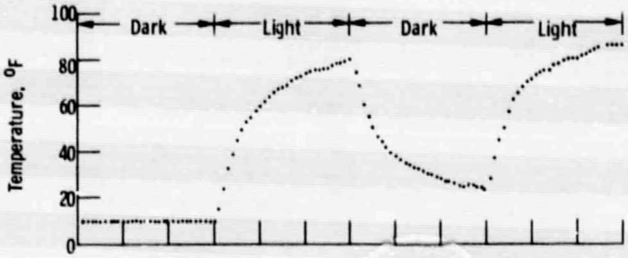

(c) Rear surface temperature as a function of time during solar simulation test of sample no. 2.

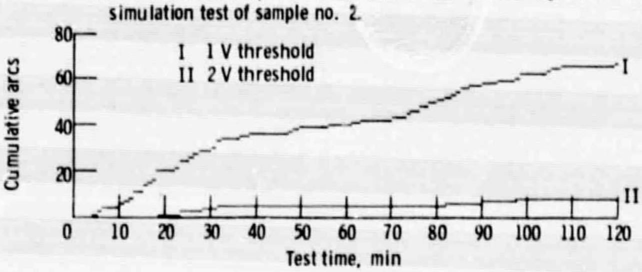

(d) Cumulative discharge count versus time during solar simulation test of sample no. 2.

Figure 8. - Concluded.

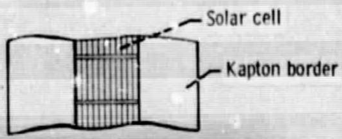

(a) Front surface potential profile, 5 KeV beam, minutes 20 and 27, 1 KV/division.

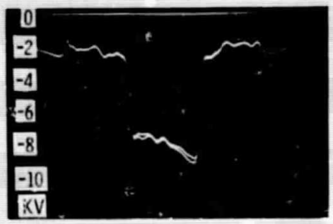

(b) Front surface potential profile, 20 KeV beam, minutes 15 and 20, 2 KV/division.

(c) Rear surface potential profile, 20 KeV beam, minute 20, 20 volt/division.

Figure 9. - Typical surface potential profiles of sample # 3.

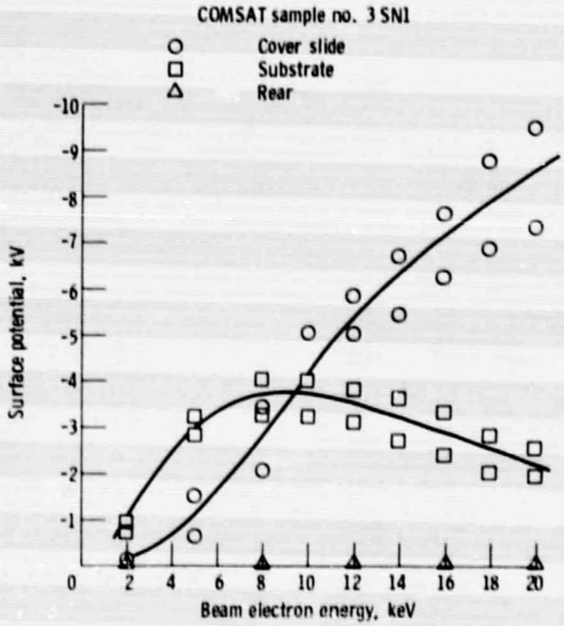

Figure 10. - Surface potential versus beam energy for sample no. 3.

ORIGINAL PAGE IS
OF POOR QUALITY

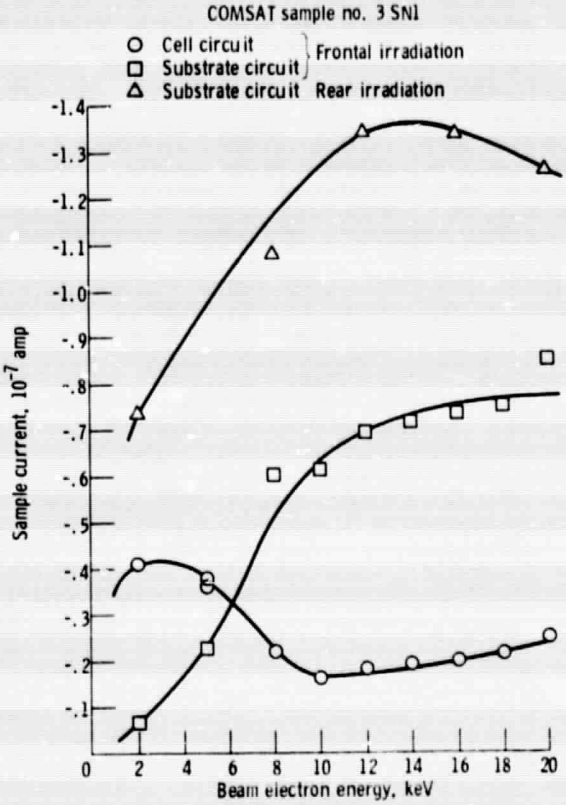

Figure 11. - Collected current versus beam energy for sample no. 3.

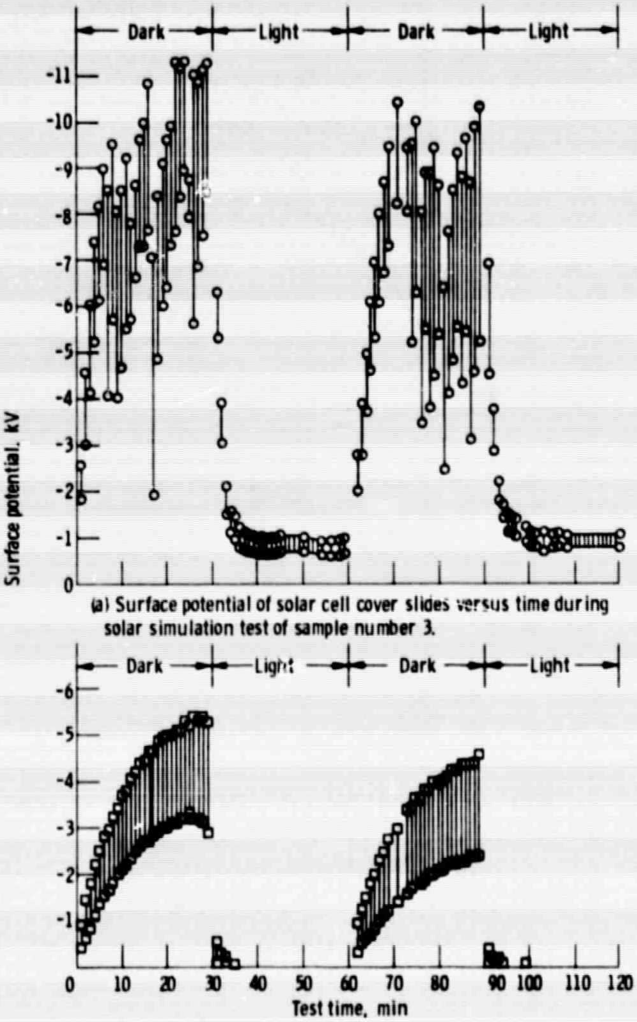

(a) Surface potential of solar cell cover slides versus time during solar simulation test of sample number 3.

(b) Surface potential of KAPTON border around solar cells versus time during solar simulation test of sample number 3.

Figure 12.

ORIGINAL PAGE IS
OF POOR QUALITY

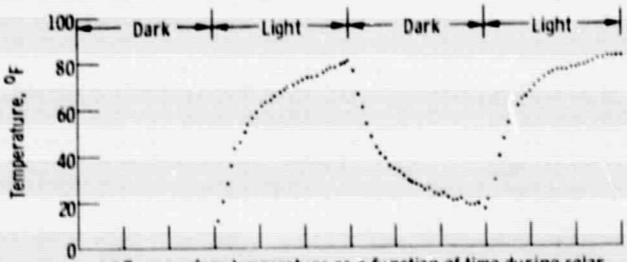

(c) Rear surface temperature as a function of time during solar simulation test of sample no. 3.

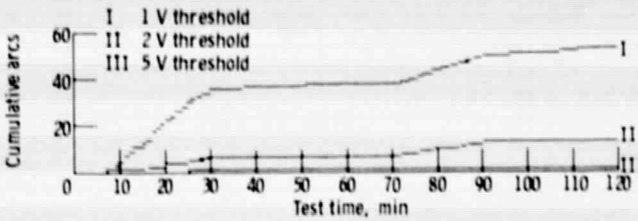

(d) Cumulative discharge count versus time during solar simulation test of sample no. 3.

Figure 12. - Concluded.

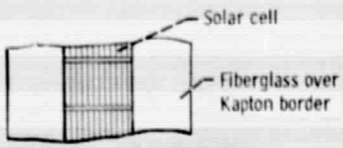

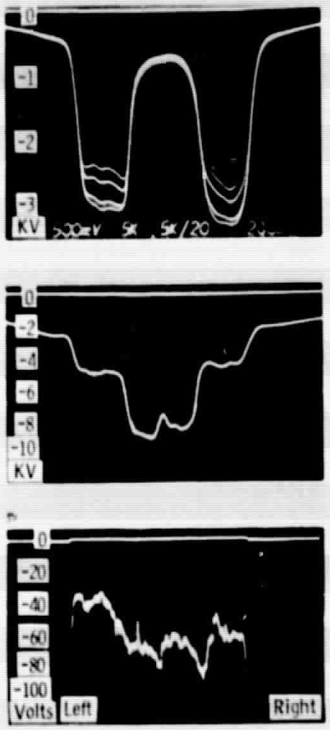

(a) Front surface potential profile, 5 KeV beam, minutes 12, 14, 18 and 20, 500 volts/division.

(b) Front surface potential profile, 20 KeV beam, minute 20, 2 KV/division.

(c) Rear surface potential profile, 20 KeV beam, minute 22, 20 volts/division.

Figure 13. - Typical surface potential profiles of sample # 4.

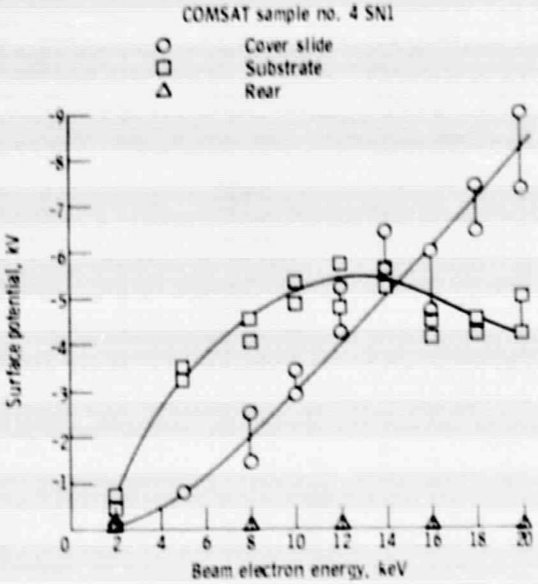

Figure 14. - Surface potential versus beam energy for sample no. 4.

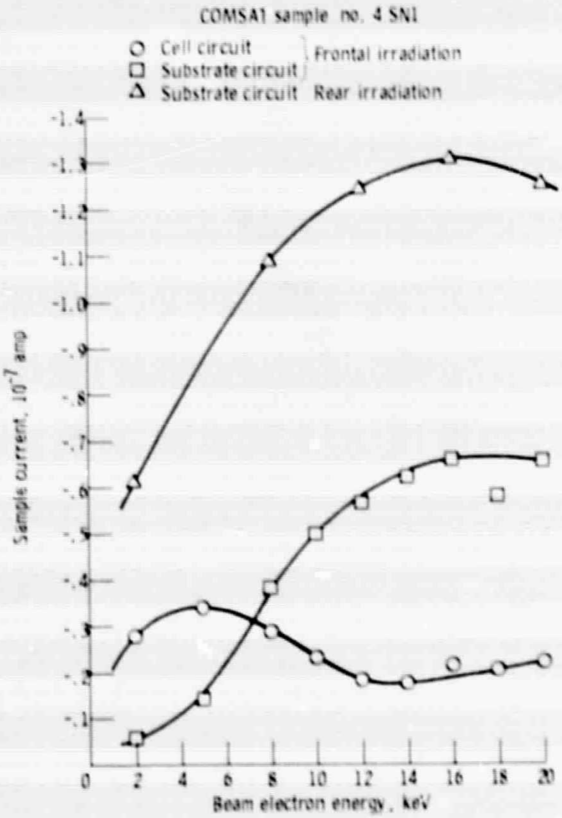

Figure 15. - Collected current versus beam energy for sample no. 4.

ORIGINAL PAGE IS
OF POOR QUALITY

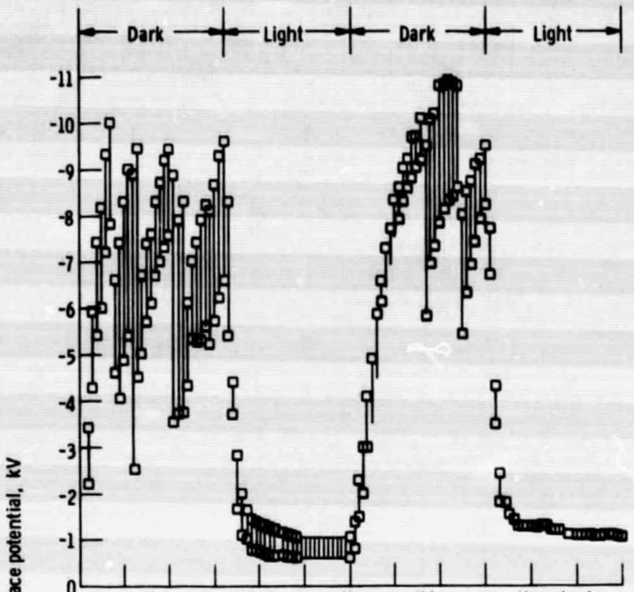

(a) Surface potential of solar cell cover slides versus time during solar simulation test of sample number 4.

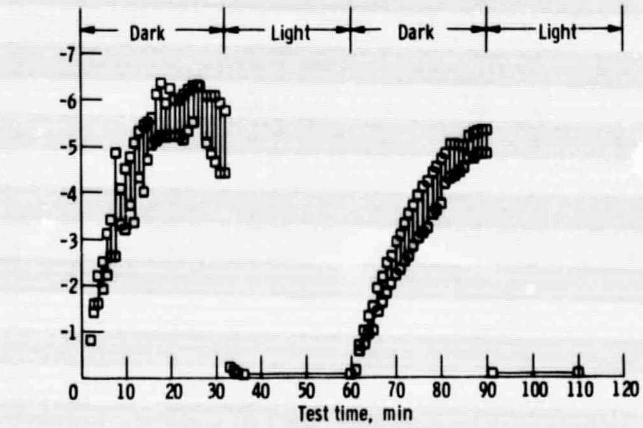

(b) Surface potential of glass fabric border around solar cells versus time during solar simulation test of sample number 4.

Figure 16.

ORIGINAL PAGE IS
OF POOR QUALITY

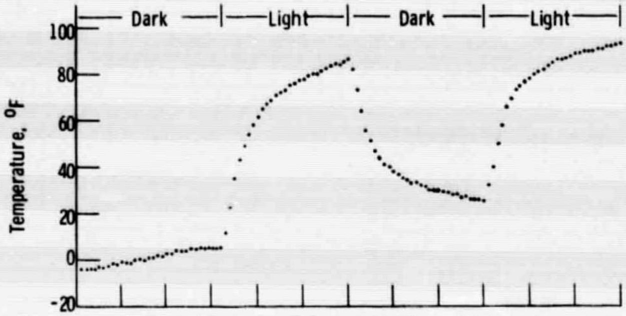

(c) Rear surface temperature as a function of time during solar simulation test of sample no. 4.

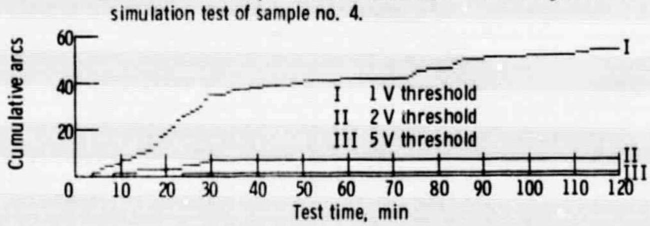

(d) Cumulative discharge count versus time during solar simulation test of sample no. 4.

Figure 16. - Concluded.

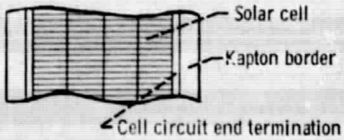

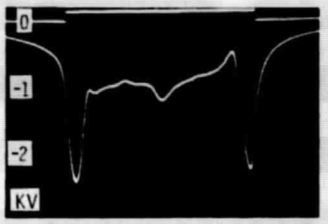

(a) Front surface potential profile, 5 KeV beam, minute 21, 500 volts/division.

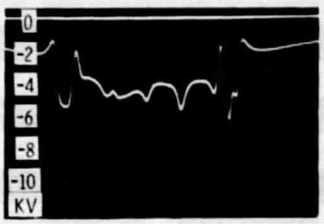

(b) Front surface potential profile, 20 KeV beam, minute 20, 2 KV/division.

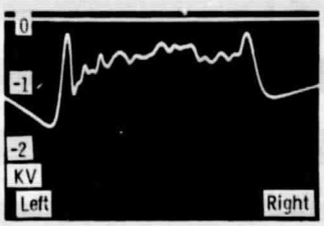

(c) Rear surface potential profile, 20 KeV beam, minute 30, 500 volts/division.

Figure 17. - Typical surface potential profiles of sample # 1.

ORIGINAL PAGE IS OF POOR QUALITY

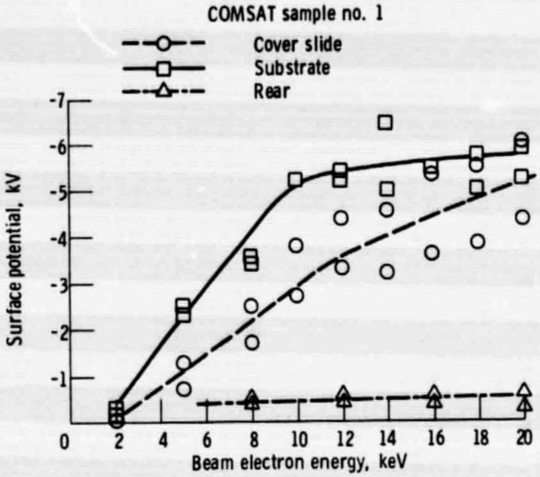

Figure 18. - Surface potential versus beam energy for sample no. 1.

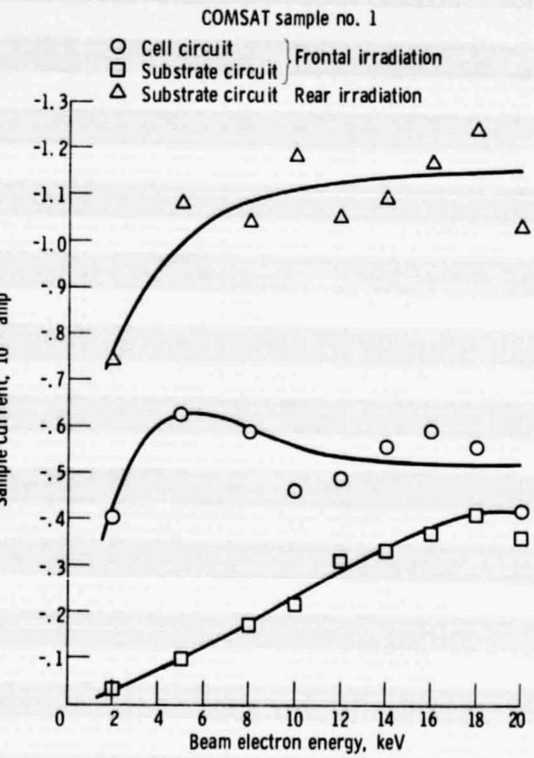

Figure 19. - Collected current versus beam energy for sample no. 1.

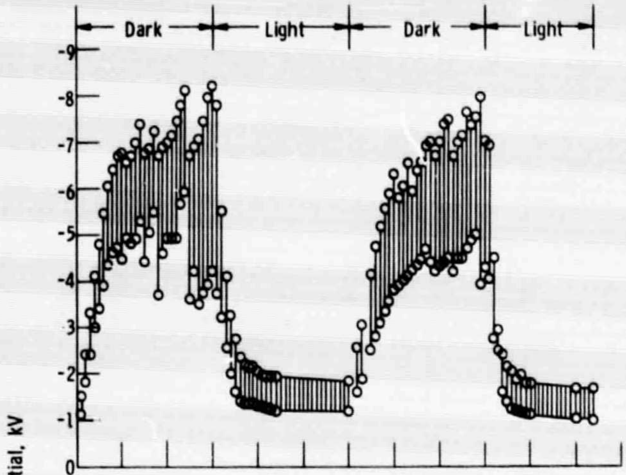

(a) Surface potential of solar cell cover slides versus time during solar simulation test of sample number 1.

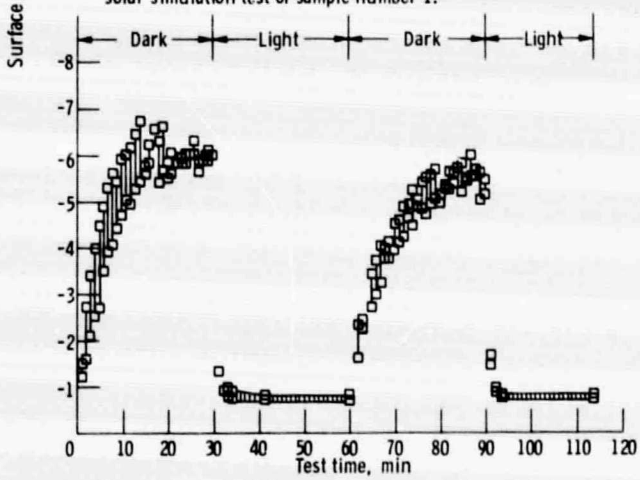

(b) Surface potential of KAPTON border around solar cells versus time during solar simulation test of sample number 1.

Figure 20.

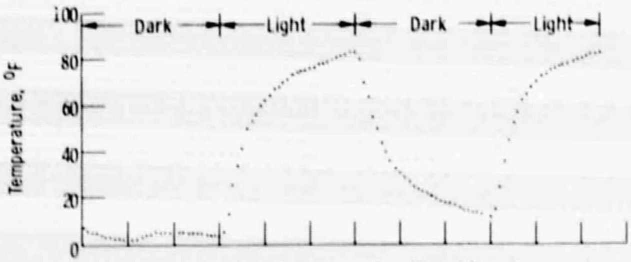

(c) Rear surface temperature as a function of time during solar simulation test of sample no. 1.

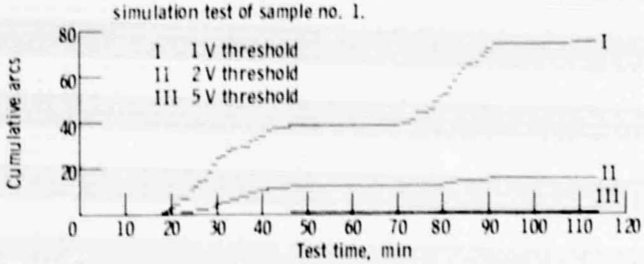

(d) Cumulative discharge count versu. time during solar simulation test of sample no. 1.

Figure 20. - Concluded.